

Li^+ ions. When the composition is changed the system passes through regions of composition where ordering fluctuations occur, leading to peaks in the "compressibility." Between the compressibility peaks the lithium form a disordered liquid. With this analogy to the thermodynamics of liquid-gas systems, it is anticipated that high-resolution and temperature-dependent electrochemical studies can be used to study the Li_xTiS_2 phase diagram in detail, including critical-exponent studies near ordered compositions.

The author thanks R. R. Chianelli, J. P. de Neufville, L. B. Ebert, A. J. Jacobson, S. C. Mraw, F. A. Putnam, B. M. Rao, B. G. Silbernagel, and M. S. Whittingham for discussions. He thanks J. R. Schrieffer for helpful suggestions and J. Kanamori and M. Kaburagi for communication of unpublished work.

¹A. H. Thompson and M. S. Whittingham, *Mater. Res. Bull.* **12**, 741 (1977).

²M. S. Whittingham, *Science* **192**, 1126 (1976), and *Solid State Chem.* **13**, 1 (1977).

³B. G. Silbernagel and M. S. Whittingham, *Mater.*

Res. Bull. **11**, 29 (1976); also A. Leblanc-Soreau, M. Danot, L. Trichet, and J. Rouxel, *Mater. Res. Bull.* **9**, 191 (1974).

⁴F. W. Boswell, A. Prodan, and J. M. Corbett, *Phys. Status Solidi (a)* **35**, 591 (1976).

⁵A. H. Thompson, F. R. Gamble, and C. R. Symon, *Mater. Res. Bull.* **10**, 915 (1975); J. J. Legendre, M. Huber, and M. Sauvage, *Phys. Status Solidi* **40**, K101 (1977).

⁶E. Rost and L. Giertsen, *Z. Anorg. Allg. Chem.* **328**, 299 (1964).

⁷B. G. Silbernagel and M. S. Whittingham, *J. Chem. Phys.* **64**, 3670 (1976).

⁸A. J. Jacobson *et al.*, to be published.

⁹M. Kaburagi and J. Kanamori, *Prog. Theor. Phys.* **54**, 30 (1975).

¹⁰M. Kaburagi and J. Kanamori, *Jpn. J. Appl. Phys., Suppl.* **2**, 145 (1974).

¹¹M. Kaburagi, Thesis, Department of Physics, Osaka University, Osaka, Japan, 1975 (unpublished).

¹²R. R. Chianelli, B. M. L. Rao, and J. Scanlon, to be published.

¹³M. S. Whittingham, *J. Electrochem. Soc.* **123**, 315 (1976).

¹⁴For example, see M. W. Zemansky, *Heat and Thermodynamics* (McGraw-Hill, New York, 1957), p. 292; or a text on chemical thermodynamics such as K. Denbigh, *The Principle of Chemical Equilibrium* (Cambridge Univ. Press, Cambridge, 1971).

Experimental Band Structure and Temperature-Dependent Magnetic Exchange Splitting of Nickel Using Angle-Resolved Photoemission

D. E. Eastman, F. J. Himpsel, and J. A. Knapp

IBM Thomas J. Watson Research Center, Yorktown Heights, New York 10598

(Received 27 March 1978)

Using angle-resolved photoemission and synchrotron radiation, we have determined the energy-versus-momentum valence-band dispersion relations for a Ni(111) crystal. The temperature-dependent ferromagnetic exchange splitting has been directly observed. Both the d -band width (~ 3.4 eV at L) and exchange splitting (0.31 eV) are much smaller than theoretical estimates (~ 4.5 eV wide at L with ~ 0.7 -eV splitting, respectively, at 293 K).

Nickel has been a prototype metal for innumerable studies of various physical properties involving itinerant-electron ferromagnetism, d -band electronic structure, and transition-metal surfaces. Despite intense study, two basic aspects of Ni have remained controversial and unresolved, i.e., the overall d -band width and the exchange splitting. For example, angle-integrated photoemission estimates of the d -band resonance width^{1,2} (~ 3.3 eV) are narrower than self-consistent one-electron band theory estimates³⁻⁵

(~ 4.5 eV). One explanation given for the observed narrow d bands is that photoemission samples only a few atomic layers and band narrowing occurs at the surface.^{6,7} Another recent explanation of the narrow experimental widths is that the lower d states in Ni have very short electron hole lifetimes.⁸ However, several recent angle-resolved photoemission experiments report larger widths (e.g., ≈ 4.2 eV)⁹ or "agree" with theory.^{10,11} Photoemission, optical, and theoretical studies of the magnetic exchange split-

ting¹² have been even more uncertain, with many experimental studies reporting negligible or unobservable splittings^{13,1,2,6} and theoretical studies³⁻⁵ typically reporting large (~ 0.6 – 0.9 eV) and uncertain splittings. Two recent angle-resolved photoemission studies have reported exchange splittings of ~ 0.3 eV¹⁰ and 0.5 eV.¹¹

Using angle-resolved photoelectron spectroscopy with linearly polarized synchrotron radiation, we have experimentally determined the energy-versus-momentum dispersion relation along the Γ - L direction in the Brillouin zone for several bands in nickel. The magnetic exchange splitting of the upper Λ_3 d band has been directly observed ($\delta E_{ex} = 0.31 \pm 0.03$ eV at 293 K). The minority $\Lambda_{3\uparrow}$ band is observed to cross the Fermi surface at $k_{\perp}/k_{BZ}^{\langle 111 \rangle} \approx 0.8$ (where k_{\perp} and $k_{BZ}^{\langle 111 \rangle}$ are the electron momentum and zone-boundary momentum), and the majority band extends from $E(\Lambda_{3\uparrow}) \approx -0.15$ eV at L to $E(\Lambda_{3\uparrow}) \approx -0.70$ eV at Γ , measured relative to the Fermi energy E_F . The temperature dependence of the exchange splitting δE_{ex} has been measured for $293 \text{ K} \lesssim T \lesssim 793 \text{ K}$. δE_{ex} is observed to decrease from 0.31 eV (293 K) to $\lesssim 0.15$ eV for $T \gtrsim T_C$ (651 K). This behavior is intermediate between long-range-order models such as a simple Stoner-Wohlfarth-Slater (SWS) model¹² which predicts that $\delta E_{ex}(T)$ varies as the magnetization, and localized intra-atomic exchange models which predict no temperature dependence. Comparison of our measured E -vs- k dispersion curves for several bands with theory^{4,5} shows that the individual d bands are theoretically about 1.4 times as wide as found experimentally. Likewise, the overall experimental width is ~ 3.4 eV (E_F to L_1), while theoretical values are^{4,5} about 4.8 eV (spin-polarized von Barth-Hedin potential and Kohn-Sham potential).

Experimentally, we have used an angle-resolved cylindrical-mirror analyzer (CMA) double-pass spectrometer system and a two-dimensional (2D) display-type spectrometer that displays the angular distribution of photoelectrons within an energy pass band ΔE and a 1.8 -sr solid angle (86° cone). The CMA system was used for s -polarization measurements and was operated with an angular acceptance $\delta\Theta = 4^\circ$ and overall energy resolution of ~ 150 meV using synchrotron radiation from the 240-MeV storage ring at the University of Wisconsin. The 2D spectrometer was used for p -polarization measurements and was operated with an angle-resolved detector set at $\delta\Theta = 4^\circ$ and an overall system resolution of ~ 100 meV using the same source. Count rates were

typically $\sim 10^4$ /sec for the Ni d bands under these conditions for $6 \lesssim h\nu \lesssim 20$ eV. Both s - and p -polarization measurements were needed to determine band symmetries and to delineate bulk and surface-state emission. In both systems, a Ni(111) crystal was prepared by Ar-ion etching and annealing in the usual manner, checked for cleanliness using Auger spectroscopy, and measured in working vacuums in the 10^{-11} -Torr range. Spectra for heated samples were taken using a pulsed heating technique with the spectrometer gated off during the heating pulse to avoid spurious magnetic fields.

In Fig. 1(a) we present an angle-resolved energy distribution curve (AREDC) which shows emission from the exchange-split uppermost d band. For the experimental conditions of Fig. 1, only the uppermost d band is observed (to be discussed). A line-shape analysis using a spin-split SWS model with two Lorentzian spectral functions of equal integrated intensity yields peaks at -0.19 and -0.47 eV with a peak splitting $\Delta_{ex} = 0.28 \pm 0.03$ eV [see Fig. 1(a)]. Because these two direct interband transitions take place at slightly different \vec{k} points, the vertical d -band exchange splitting δE_{ex} differs from Δ_{ex} by a small correction factor [equal to the ratio of d -band to conduction-band slopes of \mathcal{G} , neglecting the small effect ($\lesssim 3\%$) due to the conduction-band exchange splitting]; thus, we determine an exchange splitting $\delta E_{ex}(293 \text{ K}) = 0.31 \pm 0.03$ eV. The lower peak [≈ 0.50 eV full width at half-maximum (FWHM)] is substantially broader than the upper peak (≈ 0.30 eV FWHM) because of an increased Auger

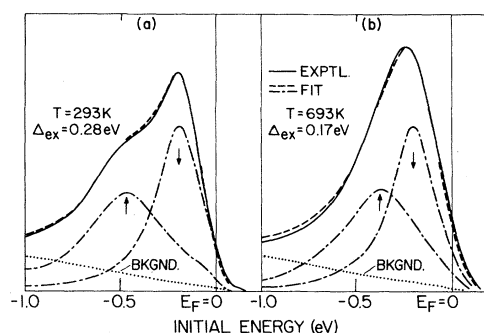


FIG. 1. AREDC's showing temperature-dependent exchange splitting $\delta E_{ex} = 1.09\Delta_{ex}$ (see text). The experimental conditions $\{h\nu = 9 \text{ eV, emission at } \Theta = 30^\circ \text{ in the } [\bar{1}\bar{1}2] \text{ direction in the } (1\bar{1}0) \text{ mirror plane with radiation polarized perpendicular to the } (1\bar{1}0) \text{ plane}\}$ ensure that only one band is observed within ~ 1 eV of E_F (see Fig. 4 inset).

lifetime broadening which increases away from E_F .

As seen in Fig. 1(b), the observed d -band line shape is narrower for $T = 693$ K (Curie point $T_C = 651$ K) than for 293 K, with the lower energy edge shifting upwards toward E_F and the peak intensity increased. This upward shift is expected since the minority band is strongly pinned with a large density of states at E_F . Using the same line-shape analysis with linewidths kept fixed yields a residual splitting of $\Delta_{ex} = 0.17$ eV, which corresponds to $\delta E_{ex}(693 \text{ K}) \approx 0.19$ eV. This result gives an upper bound for $\delta E_{ex}(693 \text{ K})$, because a line-shape analysis with any additional temperature-dependent broadening for $T \gtrsim T_C$ yields a smaller estimate.¹⁴

A summary of our experimental $\delta E_{ex}(T/T_C)$ is given in Fig. 2 (curve 1), for which an analysis with temperature-independent linewidths was used. In Fig. 2, three curves showing possible temperature-dependent exchange splittings are also shown: (2) the measured saturation magnetization $M_s(T/T_C)/M_s(0)$, which is a measure of long-range order, (3) a temperature-independent curve, which would correspond to a localized intra-atomic exchange interaction, and (4) the short-range order-parameter curve due to Oguchi¹⁵ (based on interacting localized $S = \frac{1}{2}$ moments).

We have measured normal emission AREDC's for Ni(111) with s - and p -polarized radiation for $5 \lesssim h\nu \lesssim 25$ eV, and have determined the E -vs- k_{\perp} dispersions (k_{\perp} = momentum along Λ) for the upper Λ_3 and Λ_1 d bands and the lowest Λ_1 s band. Several representative AREDC's showing direct interband transitions are given in Fig. 3, and a summary of E -vs- k_{\perp} band dispersions is given

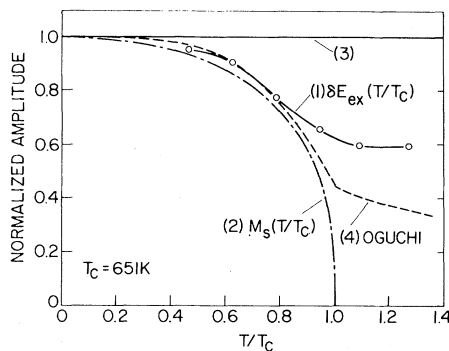


FIG. 2. Experimental temperature-dependent d -band splitting, compared with several theoretical models (see text).

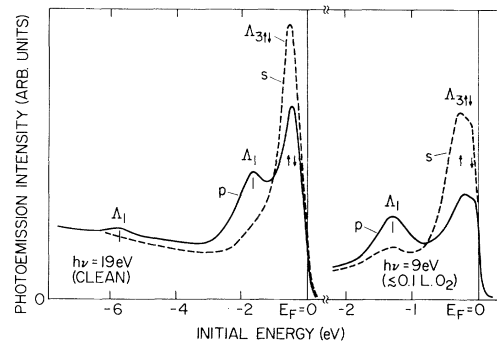


FIG. 3. AREDC's for normal emission from Ni(111) showing $h\nu$ -dependent and polarization-dependent direct interband transitions.

in Fig. 4. The E and k_{\perp} points were determined as follows: For each observed transition at a photon energy, the initial energy is directly given by the AREDC and k_{\perp} ($\pm 5\%$ accuracy) is given by that of the calculated nearly-free-electron-like Λ_1 conduction band involved¹⁶ in the transition (e.g., shown in Fig. 4 shifted down by $h\nu = 9$ eV). If we assume direct interband transitions, only one conduction band is involved for normal emission from Ni(111) with $h\nu \lesssim 20$ eV, thereby yielding unambiguous k_{\perp} assignments. In this case, transitions from Λ_1 -symmetry valence bands are allowed with p -polarized radiation (dipole approximation), while Λ_3 -symmetry bands are allowed with s polarization. The selection rules permit unambiguous assignments of experimental bands (see Fig. 3; these rules are not strictly obeyed because we have mixed s and p polarization, with $\sim 80\%$ linearly polarized radiation).

In Fig. 4, we show bands (dotted lines) calculated by Wang and Callaway using a Kohn-Sham potential.⁴ The Λ_1 bands have been spin-averaged since hole lifetimes preclude observation of the exchange splitting for $E_t \lesssim -0.5$ eV.¹⁷ As seen in Fig. 4, the theoretical width of the Λ_3 band (~ 0.8 eV), $E_F - \Lambda_{1 \text{ min}}^d$ (2.6 eV), and $E_F - L$ (4.8 eV) are all about 1.4 times as large as experimentally observed. Likewise, the calculated exchange splitting⁴ is ~ 2 – 3 times as large as measured.

In summary, we have determined dispersion relations for several bands in Ni and have observed exchange-split bands which show that ferromagnetic Ni can be described by a SWS spin-split band model. Our results are consistent with Fermi-surface results^{4,5} and spin-polarized photoemission results,¹⁸ and the exchange splitting is consistent with the Bohr magneton number

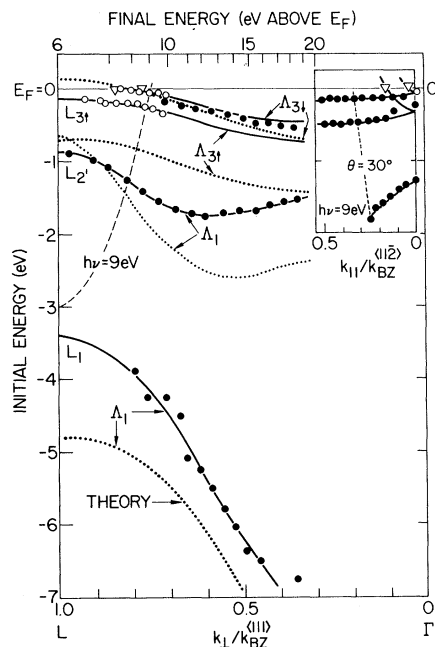


FIG. 4. Experimental E -vs- $k_L^{(111)}$ energy-band dispersions for Ni(111) along Λ . A single conduction band (Ref. 16) is involved for $h\nu \lesssim 20$ eV and is shown for $h\nu = 9$ eV (shifted down by $h\nu$). The hollow circles are data taken for Ni(111) + ~ 0.1 Torr-sec O_2 , which removes a surface state at -0.25 eV, but does not significantly affect bulk emission. The triangles denote bands crossing the Fermi surface as given by de Haas-van Alphen data (see Refs. 4 and 5; the spin-orbit splitting of Λ_{3t} is shown along Λ). The light dotted curves are calculated bands (Ref. 4) (Kohn-Sham potential). The inset shows E -vs- $k_{11}^{(112)}$ dispersion for k_{11} in the $[\bar{1}\bar{1}2]$ direction for $h\nu = 9$ eV; the dotted line $\Theta = 30^\circ$ corresponds to the data in Fig. 1(a). The zone-boundary momenta are $k_{BZ}^{(111)} = 1.55 \text{ \AA}^{-1}$ and $k_{BZ}^{(112)} = 1.46 \text{ \AA}^{-1}$.

of Ni and Stoner gap Δ .^{12,18} We find a smaller δE_{ex} and narrower d bands than given by band calculations.³⁻⁵ The discrepancy in d -band width may be related to the fact that theoretically the d -band energy position is too far above the muffin-tin zero,³ which is pinned near the bottom of the lowest Λ_1 band (see Fig. 4). Two recent studies have reported exchange splittings of $\delta E_{ex} = 0.3$ eV¹⁰ and $\delta E_{ex} = 0.5$ eV.¹¹ In the former case, one of the two observed structures was incorrectly assigned to an indirect transition from Λ_{3t} , but is due to a Λ_1 surface-state feature (to be published). In the latter case, we have observed for the same experimental parameters that the reported 0.5-eV structure ($h\nu = 16.8$ eV) is due to

two different interband transitions.

We wish to acknowledge the excellent support of the Synchrotron Radiation Center and the contributions of J. J. Donelon and V. Moruzzi. This work was supported in part by the U. S. Air Force Office of Scientific Research under Contract No. F44620-76-C-0041, and in part by the National Science Foundation under Contract No. DMR 7415089.

¹D. E. Eastman, J. Phys. (Paris) **32**, C1-293 (1971).

²S. Hufner, G. K. Wertheim, and J. H. Wernick, Phys. Rev. B **8**, 4511 (1973).

³J. W. D. Connolly, Phys. Rev. **159**, 415 (1967).

⁴C. S. Wang and J. Callaway, Phys. Rev. B **15**, 298 (1977).

⁵C. S. Wang and J. Callaway, Phys. Rev. B **9**, 4897 (1974).

⁶R. Haydock, V. Heine, M. J. Kelly, and J. B. Pendry, Phys. Rev. Lett. **19**, 868 (1972).

⁷M. Mehta and C. S. Fadley, Phys. Rev. Lett. **39**, 1569 (1977).

⁸J. B. Pendry and J. F. L. Hopkinson, in Proceeding of the Fifth International Conference on VUV Radiation Physics, Montpellier, France, 1977 (unpublished).

⁹R. J. Smith, J. Anderson, J. Hermanson, and G. J. Lapeyre, Solid State Commun. **21**, 459 (1977).

¹⁰P. Heimann and H. Neddermeyer, J. Phys. F **6**, L257 (1976).

¹¹E. Dietz, U. Gerhardt, and C. J. Maetz, Phys. Rev. Lett. **40**, 892 (1978).

¹²E. P. Wohlfarth, Phys. Lett. **36A**, 131 (1971).

¹³L. G. Petersson *et al.*, Phys. Rev. B **14**, 4177 (1976), and references therein; L. G. Petersson and R. Erlandsson, Phys. Rev. B **17**, 3006 (1978).

¹⁴However, it would require large extra broadening (~ 0.2 eV) to reduce δE_{ex} to zero for $T > T_C$. Broadening from sources of nonmagnetic origin can be ruled out because we have measured temperature-dependent line shapes for comparable transitions and temperatures in Cu and find negligible broadening. For $T/T_C \gtrsim 1$, the experimental line shape indicates that there is some additional broadening ($\gtrsim 100$ meV, possibly due to spin disorder broadening; S. Liu, private communication).

¹⁵T. Oguchi, Prog. Theor. Phys. (Kyoto) **13**, 148 (1955).

¹⁶V. Moruzzi, SCF $X\alpha$ calculation; the conduction band was shifted down by 0.5 eV to agree with experiment at L (private communication).

¹⁷We have omitted one flat d band of Λ_3 symmetry in Fig. 4 which we know from measurements on Cu(111) to have such a small emission intensity that we can not resolve it for Ni; this flat band is estimated to extend across the Brillouin zone at ~ -1.2 eV.

¹⁸E. P. Wohlfarth, Phys. Rev. Lett. **38**, 524 (1977).